Area and Volume Effects on Breakdown Strength in Liquid Nitrogen

H. Goshima, N. Hayakawa, M. Hikita, H. Okubo

Nagoya University, Nagoya, Japan

and K. Uchida

Chubu Electric Power Co. Inc., Nagoya, Japan

ABSTRACT

We measured dc and ac breakdown voltages in liquid nitrogen (LN_2) with a sphere-to-plane electrode configuration. Experimental results revealed that the breakdown voltage in LN_2 did not increase monotonously but partially decreased as the sphere diameter increased at a constant gap length. Thus, the existence of the area and the volume effects on the breakdown voltage in LN_2 was verified quantitatively; the breakdown strength decreased when increasing the $\overline{\{SEA\}}_{90}$ (90% stressed electrode area) and the $\overline{\{SLV\}}_{90}$ (90% stressed liquid volume). By changing the experimental conditions, it was verified that both area and volume effects, having a mutual correlation, simultaneously lead to the degradation of the breakdown strength in LN_2. In order to examine the area and the volume effects for the larger $\overline{\{SEA\}}_{90}$ and $\overline{\{SLV\}}_{90}$, we also measured the breakdown voltage with a coaxial cylindrical electrode. It was concluded that the dc and ac breakdown strengths in LN_2 decreased as the $\overline{\{SEA\}}_{90}$ and the $\overline{\{SLV\}}_{90}$ increased varying widely from 10^0 to 10^5 mm^2 and from 10^{-1} to 10^5 mm^3, respectively.

1. INTRODUCTION

MANY reports related to high temperature superconducting materials have appeared in the field of electric power since its discovery [1,2]. In this field, liquid nitrogen (LN_2) plays a crucial role in applying high temperature superconducting materials to the power apparatus; LN_2 is used not only as a coolant but also as an insulating material. Hence, there have been extensive studies of dielectric properties such as the breakdown voltage of LN_2 [3,4].

It is expected that high temperature superconducting power apparatus will be used at higher voltages in the future [5]. Nevertheless, most of the data on the electrical breakdown of LN_2 have been obtained under limited experimental conditions, such as small sphere-to-sphere electrodes with a small gap and relatively lower voltage levels. Thus, it is important to obtain data available for a practical insulation design of the high temperature superconducting power apparatus [6–8].

It is well known that the breakdown strength in SF_6 gas or transformer oil decreases with increasing electrode surface area or volume subjected to high electric stress [9–13]. The area and the volume effects of SF_6 gas or

1070–9878/95/$3.00

transformer oil have been statistically taken into account in the practical design of electrical insulation. An explanation is reported that these effects may be attributed to the change in the stored electrostatic field energy [14, 15]. However, scarcely any attempt has been made until now to design practical insulation for superconducting devices using LN_2. From this point of view, we have been investigating the area and the volume effects on the electrical breakdown strength in LN_2 in order to obtain the data available for designing the electrical insulation for superconducting power apparatus such as transformers, current limiters, cables and so on.

In the present paper, as the first step toward achieving the final goal, we investigate the breakdown voltage in LN_2 with sphere-to-plane and coaxial cylindrical electrode configurations. From the results, we discuss the area and the volume effects on the breakdown strength in LN_2 in terms of the 90% stressed electrode area $\overline{\{SEA\}}_{90}$ (mm^2) and the 90% stressed liquid volume $\overline{\{SLV\}}_{90}$ (mm^3).

2. EXPERIMENTAL

2.1. BREAKDOWN VOLTAGE MEASUREMENT WITH SPHERE-TO-PLANE ELECTRODE

Table 1 shows HV electrodes used for the breakdown voltage measurement in LN_2, and Figure 1 the shapes of these electrodes. The HV electrode configurations are spheres, rod and needle. A plane electrode 90 mm in diameter was used as the ground electrode for the three kinds of HV electrodes. All electrodes were made of stainless steel. The tested gap lengths were set at 0.5, 1.0 and 1.5 mm. The HV electrodes are considered to simulate five kinds of sphere electrode because the gap lengths are smaller than the sphere diameter. Accordingly, the stressed electrode area (SEA) and the stressed liquid volume (SLV) varied by changing the sphere diameter and the gap length. The surface of the sphere electrode was made either a mirror finish (roughness < 1 μm) or a rough finish (roughness ~ 70 μm).

The axis of the sphere-to-plane electrodes was placed horizontally and immersed in LN_2. The applied voltage was either a positive or negative dc ramp voltage and a 60 Hz ac ramp voltage at a rate of 5 kV/s. Under these conditions, we performed breakdown tests 50 times for each setup.

2.2. BREAKDOWN VOLTAGE MEASUREMENT WITH COAXIAL CYLINDRICAL ELECTRODE

In order to discuss the area and the volume effects with an electrode size larger than the sphere-to-plane electrode, we also measured the breakdown voltage in LN_2 with a coaxial cylindrical electrode. Figure 2 shows the coaxial cylindrical electrodes for the breakdown voltage measurement. The tested gap lengths were set at 1.0, 2.0 and 4.5 mm for the three lengths of HV electrodes. The SEA and SLV varied with the inner cylinder radius a and the effective electrode length L. All electrodes were made of stainless steel. The cylinder electrode surface had a mirror finish.

The axis of the coaxial cylindrical electrodes was placed vertically in a fiber reinforced plastic (FRP) dewar filled with LN_2. Either dc or ac voltage was applied to the inner cylindrical electrode. Under these conditions, we measured breakdown voltages 50 times for each experimental setup.

Table 1.
HV electrodes used for the breakdown measurements, for the shape, see Figure 1.

Diameter	50	20	10	6	1
Shape	sphere			rod	needle
Gap l	0.5, 1.0, 1.5				
Material	stainless steel				
Surface	mirror f. (< 1 μm), rough f. (~ 70 μm)				

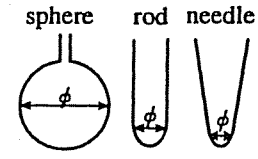

Figure 1.
Electrode shapes used in the experiments.

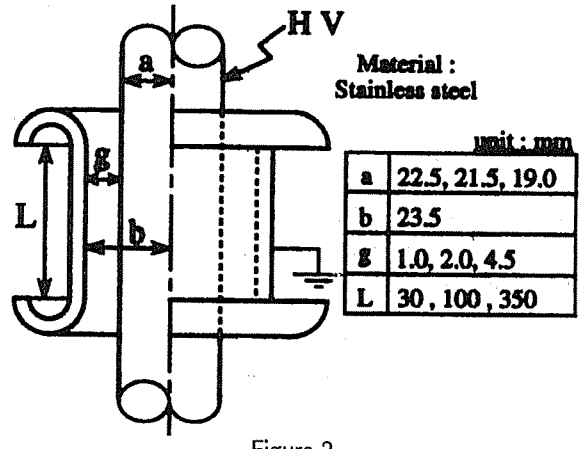

Figure 2.
Test coaxial cylindrical electrodes for the breakdown voltage measurement. a inner cylinder radius, b outer cylinder radius, g gap length, L effective electrode length.

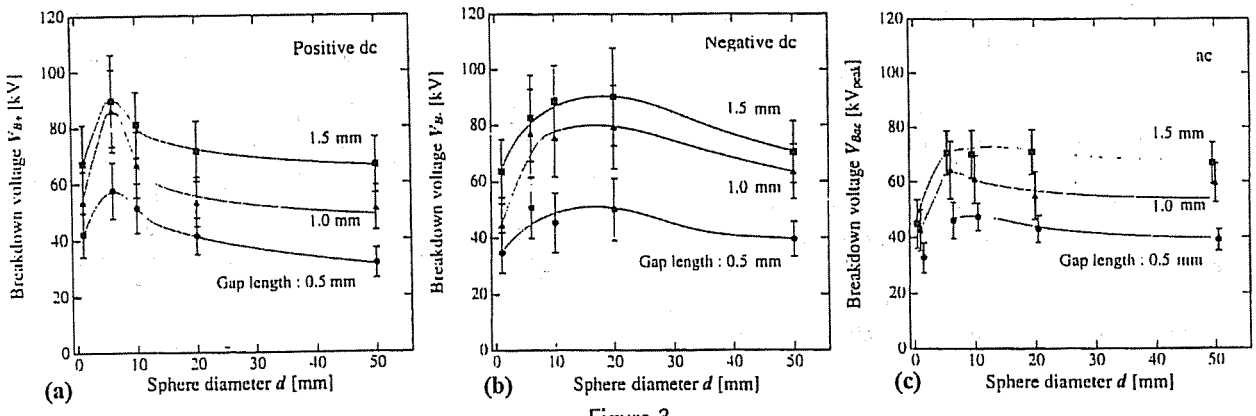

Figure 3.

Breakdown voltage in LN_2 as a function of sphere diameter d for different gap lengths. (a) Positive dc. (b) Negative dc. (c) ac.

3. RESULTS AND DISCUSSION

3.1. BREAKDOWN VOLTAGE OF LN_2 WITH SPHERE-TO-PLANE ELECTRODE CONFIGURATION

Figures 3(a) to (c) show the positive dc breakdown voltage V_{B+}, the negative dc breakdown voltage V_{B-} and the ac breakdown voltage V_{Bac} in LN_2 as a function of sphere diameter d for different gap lengths, respectively. Error bars in these Figures represent the standard deviation of breakdown voltages measured 50 times. It is found from these Figures that V_{B+} and V_{Bac} take a maximum value at $d = 6$ to 10 mm. In general, when the electrode diameter increases, the electric field distribution becomes more uniform. Thus, if the breakdown were determined only by the maximum electric field strength, the breakdown voltage would increase as the electrode diameter is enlarged. The experimental results show that the breakdown voltage decreases as the sphere diameter increases in the range of $d > 10$ mm.

Let us compare V_{B+} with V_{B-}. V_{B-} is lower than V_{B+} for $d < 10$ mm, while V_{B-} is larger than V_{B+} at $d = 20$ mm. V_{B-} is equal to V_{B+} for $d = 50$ mm. Moreover, we compare the dc breakdown voltage with ac breakdown voltage. Figure 4(a) illustrates the schematic diagram of dc and ac breakdown voltages as a function of d; the Figure is based on the experimental results shown in Figure 3. V_{Bac} seems to agree with the lower dc breakdown voltage between V_{B+} and V_{B-} for each d. Figure 4(b) shows the ratio of the number of breakdown events occurring during a positive half cycle to those during a negative half cycle in the 50 Hz breakdown tests for different sphere diameters. As seen in Figure 4(a), for $d < 10$ mm, the probability P_{B-} of the breakdown occurring during the negative half cycle is 2 to 3× as much as P_{B+} during the positive half cycle. Whereas for $d > 20$ mm, P_{B+} is larger than P_{B-} or $\approx P_{B-}$. It is worth noting that in the range of d where V_{B-} is lower than V_{B+}, P_{B-} is higher than P_{B+}; while for $d = 20$ mm, the relation is reversed; for $d = 50$ mm, $V_{B+} = V_{B-}$ and $P_{B+} \approx P_{B-}$. In other words, the polarity difference

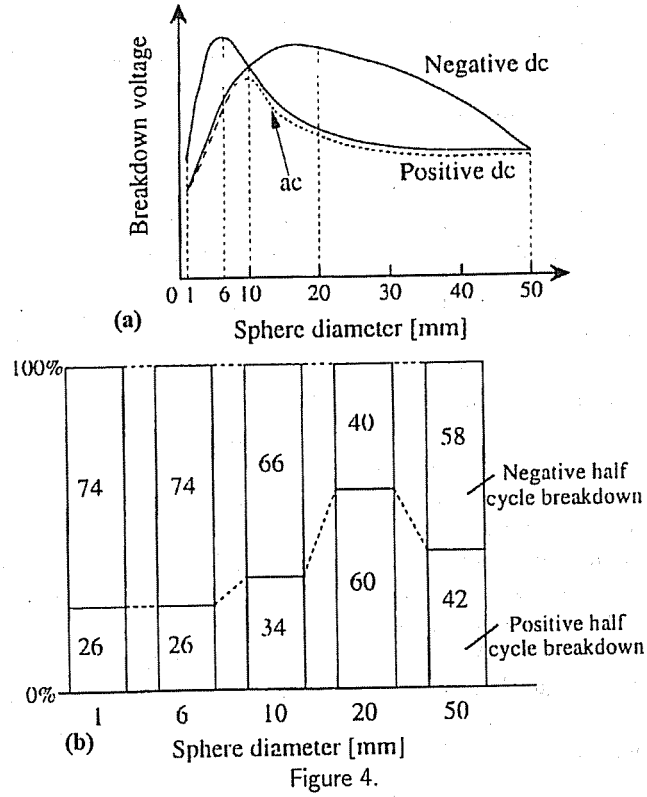

Figure 4.

Comparison between ac and dc breakdown. (a) Schematic diagram of dc and ac breakdown voltages as a function of sphere diameter. (b) The ratio of the number of breakdown events occurring during the positive half cycle to those during the negative half cycle in 50 ac breakdown tests for different sphere diameters.

between V_{B+} and V_{B-} for dc breakdown characteristics seems to be closely related to the ac breakdown properties.

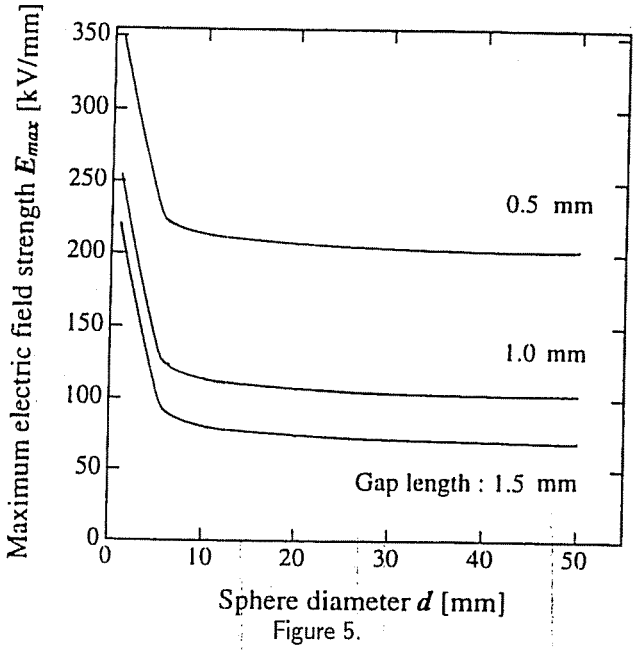

Figure 5.

Calculated maximum electric field strength E_{max} as a function of sphere diameter d for different gap lengths when 100 kV potential is assumed to be applied to the HV electrode.

3.2. ELECTRIC FIELD ANALYSIS OF SPHERE-TO-PLANE ELECTRODE CONFIGURATION

As mentioned above, the breakdown voltage in LN_2 decreased with increased sphere diameter. In other words, the breakdown voltage decreased even if the uniformity of the electric field distribution increased. To investigate the relationship between the maximum electric field strength E_{max} and the sphere diameter d, an electric field calculation was performed for the sphere-to-plane electrode configuration using the charge simulation method [16]. Figure 5 shows the calculated E_{max} as a function of sphere diameter d for different gap lengths when 100 kV potential is assumed to be applied to the HV electrode. It is obvious from this Figure that the larger d is, the lower E_{max} is. The result implies that the breakdown voltage would increase monotonically with large d because of the enhancement of the electric field uniformity if the breakdown voltage was determined by E_{max} alone. On the contrary, in our experiments, the breakdown voltage diminished as d increased. These results can be interpreted in terms of the area and the volume effects on the breakdown voltage in LN_2. Further discussion will be given in Section 3.5.

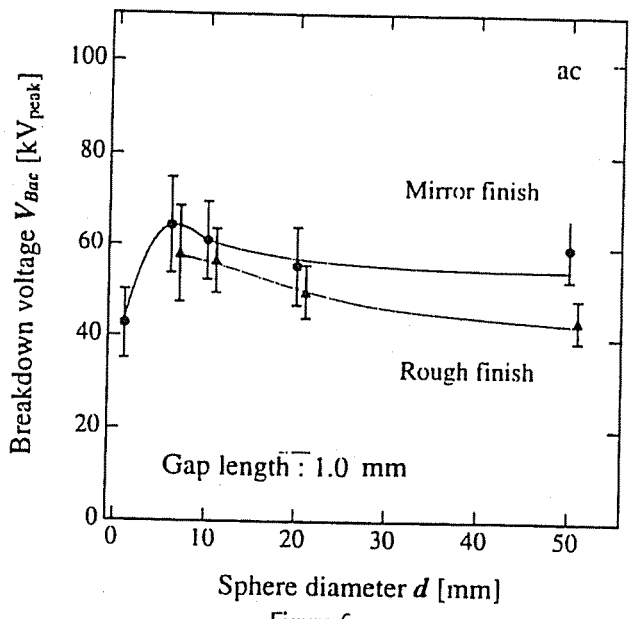

Figure 6.

ac breakdown voltage V_{Bac} in LN_2 as a function of sphere diameter d with the gap length 1 mm for different electrode surface treatments.

3.3. BREAKDOWN WITH ROUGH SURFACES

The experimental results for sphere-to-plane electrode suggested that the area and the volume effects affected the breakdown characteristics in LN_2. In order to study the area effect, we measured the breakdown voltage in LN_2 with the rough finished sphere electrode surface treatment. Figure 6 shows ac breakdown voltage V_{Bac} in LN_2 as a function of the sphere diameter d with the gap length 1 mm for different electrode surface treatments. It is evident that V_{Bac} for both mirror and rough finishes decrease as $d > 6$ mm. Moreover, V_{Bac} with the rough finish is lower than that with the mirror finish. This result may be attributed to the electron emission being enhanced with increased microscopic protrusion on the rough finished electrode surface. Thus, it can be said that there exists the area effect on V_{Bac} in LN_2. Similar results were obtained for dc voltage application.

3.4. CALCULATION OF THE $\overline{\{SEA\}}_{90}$ AND THE $\overline{\{SLV\}}_{90}$

When discussing the area and the volume effects on breakdown strength, one has to determine what should be 'area' and 'volume' affecting breakdown strength. In other words, it is necessary to determine how much a percentage of E_{max} should be considered. For instance, in the insulation design of transformers and SF_6 gas insulation systems, the electrode area and the liquid volume are usually included where the electric field exceeded 90% of E_{max}. In this paper, let us define the 'area' as the 90%

stressed electrode area ($\overline{\{SEA\}}_{90}$) and, the 'volume' as the 90% stressed liquid volume ($\overline{\{SLV\}}_{90}$).

For the sphere-to-plane electrode configuration, it is necessary to calculate the $\overline{\{SEA\}}_{90}$ and the $\overline{\{SLV\}}_{90}$ numerically, because the electric field distribution cannot be solved analytically. For the $\overline{\{SEA\}}_{90}$, the electric field strengths on the sphere and the plane electrode surfaces were calculated as well as E_{max}. The $\overline{\{SEA\}}_{90}$ was obtained as the sum of the surface area with the electric field strength $> 90E_{max}$%On the other hand, for the $\overline{\{SLV\}}_{90}$, an equifield line of 90% E_{max} was analyzed. Integrating the gap space within this equifield line allowed the estimation of $\overline{\{SLV\}}_{90}$. Thus, the calculated $\overline{\{SEA\}}_{90}$ varied from 10^{-1} to 10^{2} mm^2 and $\overline{\{SLV\}}_{90}$ from 10^{-3} to 10^{2} mm^3, respectively, for the present sphere-to-plane electrode configuration with different sphere diameters and gap lengths.

3.5. AREA AND VOLUME EFFECTS ON BREAKDOWN STRENGTH IN LN_2

3.5.1. POSITIVE dc BREAKDOWN

Figures 7(a) and (b) show the positive dc breakdown strength E_{B+} in LN_2 as a function of the $\overline{\{SEA\}}_{90}$ and the $\overline{\{SLV\}}_{90}$, respectively. Circles and triangles in the Figures represent data on the mirror finish and rough finish, respectively. It is evident from these Figures that E_{B+} decreases as the $\overline{\{SEA\}}_{90}$ or the $\overline{\{SLV\}}_{90}$ increases in a manner such that the log − log plots of E_{B+} against the $\overline{\{SEA\}}_{90}$ or the $\overline{\{SLV\}}_{90}$ are linear. Thus, these results indicate the area and the volume effects on the breakdown strength in LN_2. In these Figures, solid and dotted lines represent measured results fitted by the least squares method for the mirror finished and rough finished electrode surface treatments, respectively. Thus, obtained plots permit the expression of E_{B+} (kV/mm) as a function of the $\overline{\{SEA\}}_{90}$ and the $\overline{\{SLV\}}_{90}$ by

$$E_{B+} = 124(\overline{\{SEA\}}_{90})^{1/3.46} \quad (1)$$

$$E_{B+} = 77.1(\overline{\{SLV\}}_{90})^{1/5.62} \quad (2)$$

For the $\overline{\{SEA\}}_{90}$ and the $\overline{\{SLV\}}_{90} < 1$ mm^2 and 0.01 mm^3, respectively, E_{B+} is slightly lower than the values determined by Equation (1) and (2). For sphere diameter $d = 1$ mm, the $\overline{\{SEA\}}_{90}$ and the $\overline{\{SLV\}}_{90}$ may be comparable to the other breakdown features such as thermal bubbles, impurities and so on. Thus, the breakdown would not be determined by the area and the volume effects but by the non-uniformity of the electric field distribution. The relation between $E_{B+(R)}$ for the rough finish and the $\overline{\{SEA\}}_{90}$ was also proven to be expressed by

$$E_{B+(R)} = 108(A_{90})^{-1/3.48} \quad (3)$$

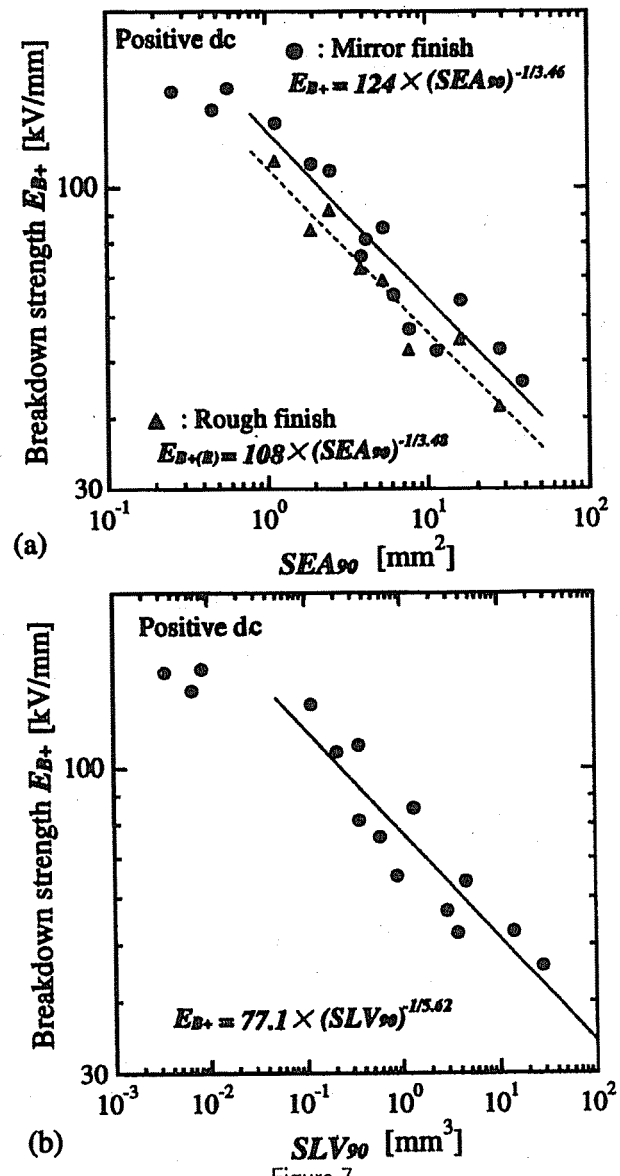

Figure 7.

Breakdown strength E_{B+} as a function of $\overline{\{SEA\}}_{90}$ and $\overline{\{SLV\}}_{90}$ for applying positive dc voltage. Circles and triangles represent data for mirror finish and rough finish, respectively. (a) Area effect. (b) Volume effect.

In Figure 7(a), the breakdown strength magnitude with the rough finish is lower compared with mirror finish, but the slope of the approximate line remains constant: $-1/3.46$ for E_{B+} is nearly equal to $-1/3.48$ for $E_{B+(R)}$. Thus, for positive dc voltage application, the roughness on the electrode surface barely affects the breakdown strength in LN_2.

3.5.2. NEGATIVE DC BREAKDOWN

Figures 8(a) and (b) show the negative dc breakdown strength E_{B-} in LN_2 as a function of the $\overline{\{SEA\}}_{90}$ and

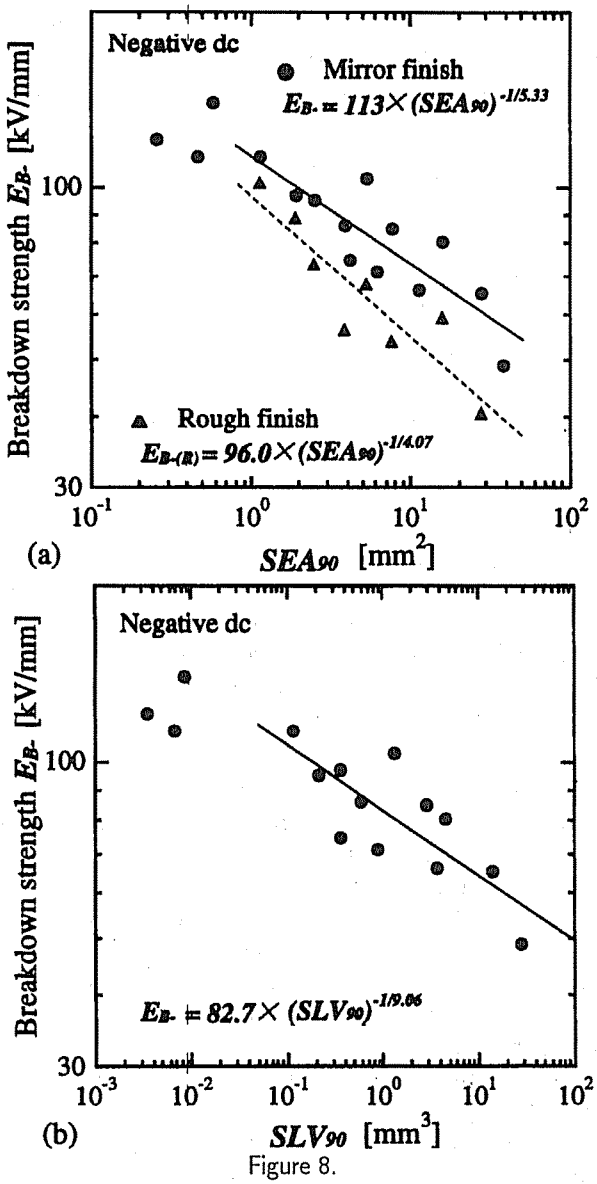

Figure 8.

Breakdown strength E_{B-} as a function of $\overline{\{SEA\}}_{90}$ and $\overline{\{SLV\}}_{90}$ for applying negative dc voltage. Symbols are the same as those in Figure 7. (a) Area effect. (b) Volume effect.

the $\overline{\{SLV\}}_{90}$, respectively. The definition of symbols is the same as that in Figure 7. It is found from these Figures that E_{B-} diminishes with the increase of the $\overline{\{SEA\}}_{90}$ or the $\overline{\{SLV\}}_{90}$, as E_{B+} does. The straight lines drawn by the least squares method allow E_{B-} to be expressed by

$$E_{B-} = 113(\overline{\{SEA\}}_{90})^{-1/5.33} \quad (4)$$

$$E_{B-} = 82.7(\overline{\{SLV\}}_{90})^{-1/9.06} \quad (5)$$

The slopes of the approximate lines for negative dc voltage application are smaller than those of positive dc case because of the polarity effect on breakdown voltage as seen in Figures 3 and 4. This polarity effect may be attributed to the difference of the electric field enhancement by charge injection effect from cathode.

For the rough finished electrode surface, $E_{B-(R)}$ is given by

$$E_{B-(R)} = 96.0(\overline{\{SEA\}}_{90})^{-1/4.07} \quad (6)$$

As seen in Figure 8(a), the rough finished treatment on the electrode surface causes the breakdown strength to decrease and the slope to be $-1/4.07$ (dotted line) steeper than $-1/5.33$ (solid line) of the mirror finish; the area effect appears more prominent for the rough finish. These results differ from the positive dc case. We interpret these results in terms of the electron emission from the rough finished cathode. For negative dc voltage, the sphere electrode becomes the cathode. Thus, the electron emission effect is significant for negative dc voltage applied to the sphere electrode with the rough finished surface treatment resulting in the enhancement of the area effect.

As seen in Figure 8(b), E_{B-} also decreases as the $\overline{\{SLV\}}_{90}$ increases. It is well known that in LN_2, thermal bubbles are likely to appear, and thus may contribute to the volume effect. Although the details of the effect of thermal bubbles on the breakdown strength are not well understood at present, this effect may be responsible for the plot of E_{B-} against the $\overline{\{SLV\}}_{90}$. Therefore, the volume effect and the area effect simultaneously lead to the degradation of the breakdown strength in LN_2.

3.5.3. ac BREAKDOWN

Figure 9 shows the ac breakdown strength E_{Bac} in LN_2 as a function of the $\overline{\{SEA\}}_{90}$ and the $\overline{\{SLV\}}_{90}$. It is seen that E_{Bac} decreases as the $\overline{\{SEA\}}_{90}$ or the $\overline{\{SLV\}}_{90}$ increases, as for the dc case. The fitted straight lines allow E_{Bac} to be expressed by

$$E_{Bac} = 96.7(\overline{\{SEA\}}_{90})^{-1/5.52} \quad (7)$$

$$E_{Bac} = 70.0(\overline{\{SLV\}}_{90})^{-1/8.62} \quad (8)$$

Moreover, $E_{Bac(R)}$ for the rough finish is given by

$$E_{Bac(R)} = 80.6(\overline{\{SEA\}}_{90})^{-1/5.23} \quad (9)$$

The rough finished surface treatment diminishes E_{Bac}, but the slope of the approximate line is unchanged in comparison with the results for the mirror finish. As a consequence, sphere surface treatment does not affect the slope of the ac breakdown characteristics, which is the same as positive dc case.

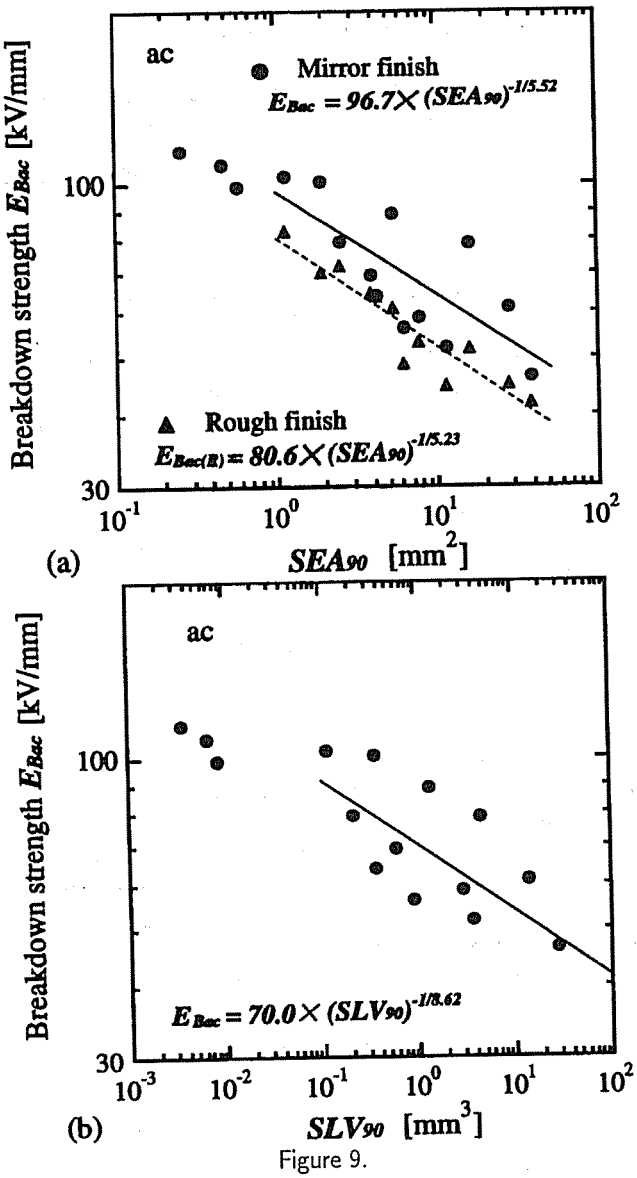

Figure 9.

Breakdown strength E_{Bac} as a function of $\overline{\{SEA\}}_{90}$ and $\overline{\{SLV\}}_{90}$ for ac voltage application. Symbols are the same as those in Figure 7. (a) Area effect. (b) Volume effect.

3.6. BREAKDOWN WITH COAXIAL CYLINDRICAL ELECTRODE CONFIGURATION

Since one can obtain an electric field distribution analytically for a coaxial cylindrical electrode configuration, the $\overline{\{SEA\}}_{90}$ and the $\overline{\{SLV\}}_{90}$ shown in Section 3.4 can be calculated as follows. A maximum electric field strength E_{max} for the coaxial cylindrical electrode is given by

$$E_{max} = \frac{V}{a \ln(b/a)} \tag{10}$$

where V is the applied voltage, a and b are the inner and the outer cylinder radii, respectively. The $\overline{\{SEA\}}_{90}$ and the $\overline{\{SLV\}}_{90}$ derived from Equation (10) are given in Equation (11) and (12)

$$\overline{\{SEA\}}_{90} = \begin{cases} 2\pi La & a < 0.9b \\ 2\pi L(a+b) & a \geqslant 0.9b \end{cases} \tag{11}$$

$$\overline{\{SLV\}}_{90} = \begin{cases} \frac{19}{81}\pi La^2 & a \leqslant 0.9b \\ \pi L(b^2 - a^2) & a \geqslant 0.9b \end{cases} \tag{12}$$

where L is the effective electrode length. In Equations (11) and (12), the $\overline{\{SEA\}}_{90}$ and $\overline{\{SLV\}}_{90}$ for $a \geqslant 0.9b$ correspond to the whole electrode surface area and the gap space, respectively, because the electric field strength on the outer cylindrical electrode reaches 90% of E_{max}.

Thus, the present coaxial cylindrical electrodes allowed the $\overline{\{SEA\}}_{90}$ and the $\overline{\{SLV\}}_{90}$ to vary from 10^3 to 10^5 mm^2 and from 10^3 to 10^5 mm^3, respectively. Thus, using both the sphere-to-plane and the coaxial cylindrical electrode configurations, we can discuss the area and volume effects in LN_2 over the wide range from 10^0 to 10^5 mm^2 and from 10^{-1} to 10^5 mm^3.

Figures 10(a) and (b) show ac breakdown strength E_{Bac} in LN_2 as a function of $\overline{\{SEA\}}_{90}$ and the $\overline{\{SLV\}}_{90}$ for different electrode configurations. From these Figures we found also that E_{Bac} decreases to 1/5 when the $\overline{\{SEA\}}_{90}$ and the $\overline{\{SLV\}}_{90}$ increase from 10^0 to 10^5 mm^2 and from 10^{-1} to 10^5 mm^3, respectively. It should be emphasized that the extrapolation of the least squared fit straight line for the sphere-to-plane electrodes also fits the data for the coaxial cylindrical electrodes. In other words, the area and the volume effects on the breakdown strength in LN_2 are continuous over 5 and 6 decades of the $\overline{\{SEA\}}_{90}$ and the $\overline{\{SLV\}}_{90}$. We have also confirmed that the breakdown characteristics in LN_2 for dc voltage application are similar to those for ac case.

4. CONCLUSION

WE measured dc and ac breakdown voltages in LN_2 with the sphere-to-plane and the coaxial cylindrical electrode configurations. From the experimental results, we examined the area and the volume effects on the breakdown strength in LN_2.

The experimental results showed that dc and ac breakdown voltages did not increase monotonically but partially decreased as the sphere diameter increased beyond 10 mm while keeping the gap length constant. To discuss the results quantitatively, we introduced the $\overline{\{SEA\}}_{90}$ (90% stressed electrode area) and the $\overline{\{SLV\}}_{90}$ (90% stressed liquid volume). It was found that dc and ac breakdown strengths in LN_2 decreased as the $\overline{\{SEA\}}_{90}$ or the $\overline{\{SLV\}}_{90}$ increased on the log – log scale. Both the

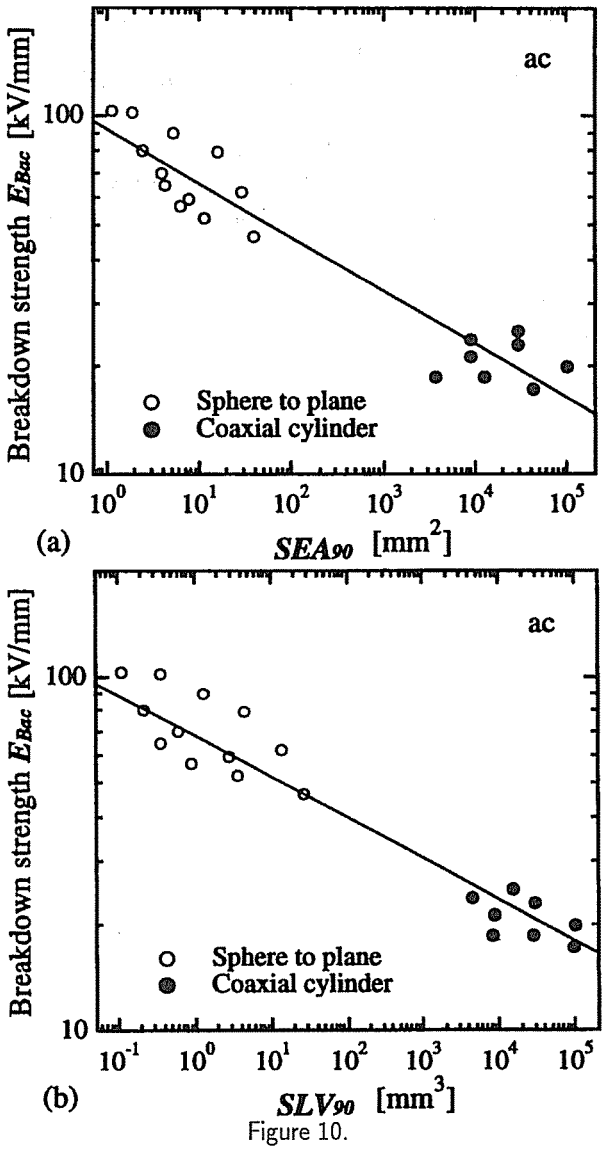

Figure 10.

ac breakdown strength E_{Bac} as a function of $\overline{\{SEA\}}_{90}$ and $\overline{\{SLV\}}_{90}$ for different electrode configurations. (a) Area effect. (b) Volume effect.

area effect and the volume effect caused the degradation of the breakdown strength in LN_2.

In positive dc and ac voltage applications, the roughness on the electrode surface had little influence on the breakdown strength in LN_2. On the other hand, in applying negative dc voltage, the rough finished treatment on the electrode surface decreased the breakdown strength, and made the slope of the area effect steeper than that for the mirror finish; the area effect appeared more prominent for the rough finish. These results indicate that electron emission from the rough finished cathode affected the breakdown strength for negative dc voltage application.

The area and the volume effects on the breakdown strength in LN_2 appeared in the wide range of value from 10^0 to 10^5 mm^2 for the $\overline{\{SEA\}}_{90}$ and from 10^{-1} to 10^5 mm^3 for the $\overline{\{SLV\}}_{90}$, respectively. Experimental results revealed that dc and ac breakdown strengths in LN_2 would decrease to 1/5 of the value as the $\overline{\{SEA\}}_{90}$ or the $\overline{\{SLV\}}_{90}$ increase.

REFERENCES

[1] G. Begin, P. R. Critchlow and R. Roberge, "Technological Impact Study of Superconductivity at Liquid Nitrogen Temperature for an Electric Utility", Conf. Elect. Appl. of Superconductivity, 1988.

[2] F. Y. Chu, "Application of High Temperature Superconducting Materials in the Electric Power System-an Ontario Hydro Perspective", World Congress on Superconductivity, Houston, pp. 129–138, 1988.

[3] M. Hara, T. Kaneko and K. Honda, "Thermal-bubble Initiated Breakdown Characteristics of Liquid Helium and Nitrogen at Atmospheric Pressure", IEEE Trans. EI, Vol. 23, No. 4, pp. 769–778, 1988.

[4] M. Hara D. J. Kwak and M. Kubuki, "Thermal Bubble Breakdown Characteristics of LN_2 at 0.1 MPa under ac and Impulse Electric Fields", Cryogenics, Vol. 29, pp. 895–903, 1989.

[5] E. B. Forsyth, "The High Voltage Design of Superconducting Power Transmission Systems", IEEE Electrical Insulation Magazine, Vol. 6, No. 4, pp. 7–16, 1990.

[6] R. J. Meats, "The Impulse Voltage Flashover of Dielectric Spacers in a Helium-insulated Superconducting Cable Model", Cryogenics, Vol. 16, pp. 77–80, 1977.

[7] J. Gerhold, "Electrical Insulation in Superconducting Power Systems", IEEE Electrical Insulation Magazine, Vol. 8, No. 3, pp. 14–20, 1992.

[8] J. Gerhold and M. Hara, "Procedure of Electrical Insulation Design for Superconducting Coils", Proc. of 8th ISH, 93.04, pp. 567–570, 1993.

[9] P. J. Sinz, *Influence of Moisture and Particles on the Electric Strength of Insulating Oils*, Doctor thesis of the Technical University of Graz, 1990.

[10] Y. Kawaguchi, H. Murata and M. Ikeda, "Breakdown of Transformer Oil", IEEE Trans. PAS, Vol. 91, No. 9, pp. 9–23, 1972.

[11] M. Ikeda, T. Teranishi, M. Honda and T. Yanari, "Breakdown Characteristics of Moving Transformer Oil", IEEE Trans. PAS, Vol. 100, No. 2, pp. 921–928, 1981.

[12] C. Korasli, I. C. Somerville and O. Farish, "Electrode-area and Surface-roughness Effects on Breakdown of SF_6/N_2 Mixture", *Gaseous Dielectrics II*, p. 218, 1980.

[13] A. Rein and J. Kulstas, "Impulse Breakdown of SF_6/N_2 Insulation. Influence of Electrode Covering. Polarity Effects", *Gaseous Dielectrics III*, p. 315, 1982.

[14] J. D. Cross, "A Physical Explanation of the Effects of Electrode Area on the Breakdown of Liquid Dielectrics", Canadian Electrical Engineering Journal, Vol. 7, No. 2, pp. 28–30, 1982.

[15] B. Mazurek and J. D. Cross, "An Energy Explanation of The Area Effect on Electrical Breakdown in Vacuum", IEEE Trans. EI, Vol. 22, No. 3, pp. 341–346, 1987.

[16] H. Singer, H. Steinbigler and P. Weiß, "A Charge Simulation Method for the Calculation of High Voltage Fields", IEEE Trans. PAS, Vol. 93, No. 5, pp. 1660–1668, 1974.

Manuscript was received on 2 July 1994, in revised form 25 January 1995.